Green Chemistry

Silane Diamine Copolymers: Efficient Synthesis, Solvent Absorption Capacity, and Limitations as Coatings

Journal:	*Green Chemistry*
Manuscript ID	GC-ART-01-2024-000404.R1
Article Type:	Paper
Date Submitted by the Author:	02-Mar-2024
Complete List of Authors:	Nguyen, Thao; Arizona State University, School of Molecular Sciences Sharma, Anuja; Arizona State University, School of Molecular Sciences Le Phuong Nguyen, Tam; Arizona State University, School of Molecular Sciences Trimble, Michael ; Arizona State University, School of Molecular Sciences Seo, Dong-Kyun; Arizona State University, School of Molecular Sciences Trovitch, Ryan; Arizona State University, School of Molecular Sciences

PAPER

Silane Diamine Copolymers: Efficient Synthesis, Solvent Absorption Capacity, and Limitations as Coatings

Received 00th January 20xx,
Accepted 00th January 20xx

DOI: 10.1039/x0xx00000x

Thao T. Nguyen, Anuja Sharma, Tam Le Phuong Nguyen, Michael A. Trimble, Dong-Kyun Seo and Ryan J. Trovitch*

Although silane diamine copolymers have captured the attention of the catalysis community, the optimization of their synthesis and end uses have yet to be explored. In this study, a well-defined Earth-abundant metal catalyst, [(2,6-*i*Pr$_2$Ph BDI)Mn(μ-H)]$_2$, has been found to couple organosilanes to diamines to prepare networks that feature varied silane substitution and diamine chain lengths. By performing dehydrocoupling in the absence of solvent with 0.01 mol% catalyst loading, substrate utilisation turnover frequencies of up to 300 s^{-1} have been achieved at early reaction times, the highest Si–N dehydrocoupling activity ever observed. These networks have been employed as absorbents for common organic solvents, a property that had not been studied for this class of materials. By incorporating a long-chain hydrophobic linker, one network has been found to absorb 7.7× its orginal mass in THF and recycling has been demonstrated upon solvent removal. Controlling the degree of dehydrocoupling also offered an opportunity to deposit coatings from freshly-prepared silane diamine polymer solutions and monitor their integrity upon curing in air. While uniform and persistent coatings have been obtained from 1,6-hexanediamine derived polymers, the need to prepare dilute solutions that have a short shelf-life and the tackiness associated with extended dry times have been identified as potential limitations.

Introduction

Polymers possessing Si–N bonds are of industrial importance since they can be used to deposit coatings that exhibit chemical and thermal stability.[1] Thin films of Si_3N_4, SiO_xN_y, SiC_xN_y, and $SiC_xN_yO_z$ can be obtained by tuning the precursor composition and curing conditions,[2] and they serve as excellent protective layers for microelectronics, photonic devices, and solar cells.[3,4] Organopolysilazanes, which feature Si–N–Si linkages and organic functionality on silicon (**Fig. 1**, a), allow for the fine-tuning of performance properties.[5] Once applied to a surface, they can be cured by moisture at ambient temperature to yield dense amorphous coatings.[6] This property renders them ideal for situations where thermal curing is not suitable, such as the application of anti-fouling, anti-graffiti, and non-stick coatings for weather protection.[7,8]

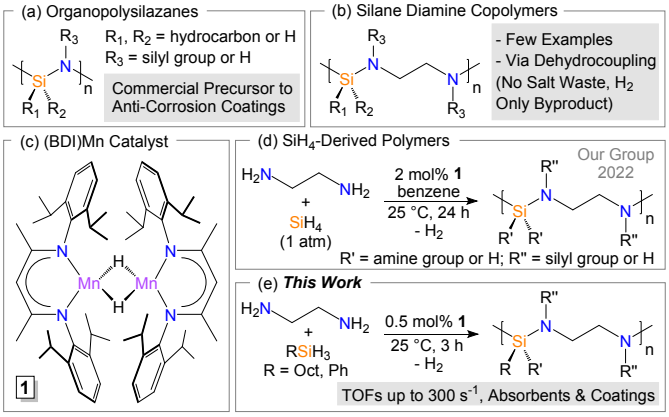

Fig. 1 Strategy for the efficient preparation of silane diamine copolymers and their evaluation for subsequent applications.

Silane diamine copolymers (**Fig. 1**, b; sometimes referred to in the literature as polycarbosilazanes) are structurally related to organopolysilazanes; however, their reactivity and use for subsequent applications have been considerably less explored. In 1968, Fink demonstrated that compounds of this type could be prepared via the dehydrocoupling of secondary silanes with diamines.[9] This approach to Si–N bond formation is preferable to traditional chlorosilane amination,[10,11] in that it leads to higher molecular weight polymers,[12] avoids the use of corrosive reagents, and affords hydrogen as a byproduct rather than a stoichiometric amount of ammonium salt waste.[13]

Following Fink's discovery, silane diamine polymers were overlooked until $Ba[CH(SiMe_3)_2]_2(THF)_3$ was shown to catalyse

[a] School of Molecular Sciences, Arizona State University, Tempe, AZ 85287, USA. E-mail: ryan.trovitch@asu.edu

Electronic Supplementary Information (ESI) available: General considerations, detailed procedures, and characterization data. See DOI: 10.1039/x0xx00000x

diphenylsilane and *p*-xylylenediamine dehydrocoupling at 60 °C in 2016.[14,15] A related catalyst, $Ba[N(SiMe_3)_2]_2(THF)_2$, was then used to prepare ferrocene-containing silane diamine polymers which were pyrolysed to afford magnetic ceramic materials.[16] In 2020, Webster reported phenylsilane and *p*-xylylenediamine coupling using the β-diketiminate (BDI) iron catalyst, $[(^{2,6\text{-}i\text{Pr}_2\text{Ph}}\text{BDI})\text{Fe}(\mu\text{-H})]_2$.[17] Last year, silicon-stereogenic variants were synthesized using an *in situ* generated rhodium catalyst.[18] Our group subsequently demonstrated that the aryl diimine (ADI) cobalt catalyst, $(^{\text{Ph}_2\text{PPr}}\text{ADI})\text{Co}$, can dehydrocouple diamines and hydrosiloxanes with turnover frequencies (TOFs) of up to 157 s^{-1} relative to substrate.[19] Prior to this study, the highest activity for Si–N dehydrocoupling was 91.7 s^{-1}, reported for the *N*-heterocyclic carbene complex, $[Pt(I^tBu')(I^tBu)][BAr^F_4]$.[13,20]

In 2018, our group reported the synthesis of the manganese hydride dimer, $[(^{2,6\text{-}i\text{Pr}_2\text{Ph}}\text{BDI})\text{Mn}(\mu\text{-H})]_2$ (**1**, **Fig. 1**, c), and its ability to mediate olefin hydrosilylation.[21] Electronic structure analysis revealed that this dimer readily overcomes the 1.5 kcal/mol barrier required to dissociate into monomers,[22] a feature that allows the manganese centres to enter a catalytic cycle.[21,23,24] Notably, this catalyst has been found to promote N–H activation and subsequent Si–N dehydrocoupling to afford aminosilane CVD precursors, perhydropolysilazane, and silane diamine copolymers when using SiH_4 as the coupling partner (**Fig. 1**, d).[24] With knowledge of this activity as a starting point, this study commences with the preparation of two previously undescribed sets of silane diamine polymer networks via **1**-catalysed Si–N dehydrocoupling (**Fig. 1**, e). By lowering the catalyst loading and monitoring conversion, diamine silylation TOFs of up to 300 s^{-1} are observed, the highest activity to be noted for this reaction. These networks are identified as scavengers of organic solvents for the first time, capable of swelling to several times their initial mass. Since silane diamine copolymers are known to hydrolyse in the same way that commercial organopolysilazanes do, we hypothesized that controlling the degree of crosslinking could allow for their application as coatings that cure in air. This possibility has recently appeared in the patent literature,[25,26] and this contribution aims to more thoroughly highlight the promise and potential limitations of silane diamine coatings.

Results and discussion

Preparation of Silane Diamine Networks. Knowing that **1** is active for Si–N dehydrocoupling at room temperature,[24] its use to synthesize new organosilane diamine copolymers was evaluated. Adding an equimolar mixture of ethylenediamine and phenylsilane to 0.5 mol% of **1** in the absence of solvent resulted in the immediate and vigorous loss of H_2 and darkening of the solution from yellow to dark brown within 3 h (the reaction was left open to N_2 atmosphere to prevent the buildup of pressure). When conducted in the presence of mesitylene as an internal standard, ^{1}H NMR analysis of the solution revealed greater than 99% ethylenediamine utilization (for optimization, see **Table S1**). Repeating this procedure in the absence of mesitylene, quickly exposing the product to air to deactivate the catalyst, washing with pentane and diethyl ether, and drying *in vacuo* afforded **1a** (**Table 1**) as a solid in 72% isolated yield.

Table 1 Dehydrocoupling of diamines to $PhSiH_3$ using 0.5 mol% of **1** to prepare silane diamine networks.

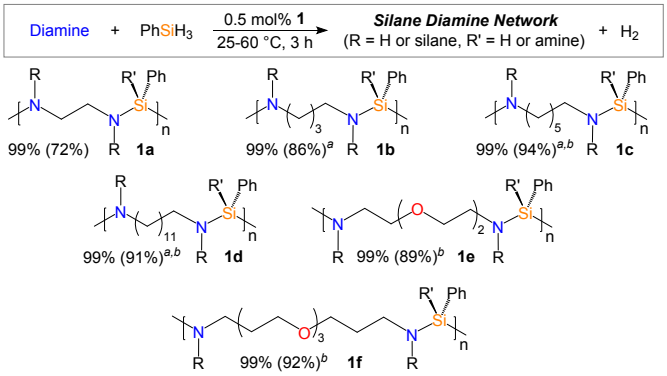

Percent conversion (99%) determined by ^{1}H NMR integration of unreacted diamine. Isolated yields shown in parentheses. [a] Trial conducted in 2 mL of benzene-d_6. [b] Trial conducted for 3 h at 60 °C.

The IR spectrum of **1a** features a broad N–H stretch at 3372 cm^{-1}, a modest Si–H stretch at 2119 cm^{-1}, and a weak Si–N stretch at 830 cm^{-1} (**Fig. S3**).[27] The observation of N–H and Si–H peaks indicates that the R and R' substituents of **1a** are often H. However, this product must also feature considerable crosslinking (i.e., where R = silane and R' = amine) since a solid is obtained, rather than a linear oil.[19] The instability of silane diamine networks towards protic solvents and their insolubility in common organic solvents precluded bulk NMR and molecular weight analysis.[24] However, after soaking **1a** in THF, MALDI-TOF MS analysis of the wash revealed Gaussian distributions ranging from 329 to 3079 g/mol. These peaks are consistent with residual 2- to 18-unit oligomers of **1a** being extracted from the bulk material. Soaking freshly prepared **1a** in benzene-d_6 allowed for the observation of broad resonances attributed to the same oligomers by ^{1}H NMR spectroscopy (for a representative spectrum, see **Fig. S2**).

The diamine chain length was then varied from C_2 to C_{12} (**1a**-**1d**) and diamines containing ether functional groups were also polymerized (**1e**, **1f**). Because they exist as solids at ambient temperature, the dehydrocoupling of 1,4-diaminobutane, 1,6-diaminohexane, and 1,12-diaminododecane was performed in 2 mL of benzene-d_6. The synthesis of **1c**-**1f** required heating to 60 °C (**Table S1**), possibly due to the lower concentrations of amine present, affording the corresponding silane diamine network in good yield (89-94%). As observed for **1a**, compounds **1b**-**1d** were found to exhibit IR spectra consistent with the presence of N–H, Si–H, and Si–N bonds. The IR spectra of **1e** and **1f** did not feature Si–H stretching, suggesting a higher level of crosslinking. This may be due to the steric bulk of the ligand in **1**, which may allow long chain amines to access the metal while preventing the activation of amines adjacent to the bulk material. The diamine scope was purposely limited to lightly-functionalized substrates that are produced on scale; however, catalyst **1** tends to reduce unsaturated functional groups including alkenes,[21] carbonyls,[21,23] and nitriles[23] and is known to be tolerant of phosphines[21,23] and halogens[23] under conditions similar to those of **Table 1**.

Octylsilane dehydrocoupling was then evaluated to prepare networks that feature aliphatic substitution. Using 0.5 mol% of **1** and the same set of conditions, product formation was noted for each trial in Table 2 after 3 h at 25 °C (**2a**-**2b**) or 60 °C (**2c**-**2f**). In the absence of mesitylene internal standard, **2a**-**2f** were isolated as solids in good yield (77-94%) and were confirmed to feature amine and hydrosilane moieties by IR spectroscopy. As observed for the products in **Table 1**, MALDI-TOF MS analysis revealed oligomeric fragments with molecular weights of up to 2850 g/mol (**Table 3**).

Table 2 Dehydrocoupling of diamines to $OctSiH_3$ using 0.5 mol% of **1** to prepare silane diamine networks.

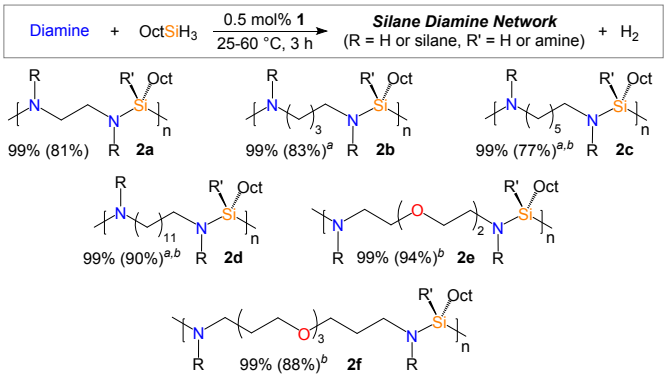

Percent conversion (99%) determined by ^{1}H NMR integration of unreacted diamine. Isolated yields shown in parentheses. [a] Trial conducted in 2 mL of benzene-d_6. [b] Trial conducted for 3 h at 60 °C.

Product Stability. Considering the propensity of silane diamine polymers to hydrolyse,[13,24] the curing of **1a** was monitored upon exposure to air featuring 27% humidity. Notably, this compound began to harden and turn white in colour in as little as 1 min (**Fig. 2**). Over the course of 24 h, a bright white siloxane featuring trifunctional (T) branching groups had formed, and a colourless liquid had condensed around the material. This liquid was confirmed to be ethylenediamine by NMR spectroscopy, which had been released in favor of Si–O–Si bond formation. Accordingly, monitoring this process by FT-IR spectroscopy revealed a significant decrease in Si–H and Si–N vibration absorbance over the course of 24 h, followed by the appearance of an Si–O vibration (**Fig. S63**). Products **1a** and **2a**, which feature ethylenediamine linkers, were observed to hydrolyse considerably faster than the networks featuring longer chain diamines, which impart greater hydrophobicity.[19]

Simultaneous thermal analysis was then performed to examine the thermal stability of each solid. In one set of experiments, samples of **1a-1f** and **2a-2f** were sealed within vials under N_2, removed from the glovebox, and loaded onto a Mettler Toledo balance as quickly as possible to perform thermogravimetric analysis (TGA) with differential scanning calorimetry (DSC) under N_2 (**Table 3**). Analogously, a second set of experiments collected TGA-DSC data under O_2 while limiting exposure to moisture in air. The products were generally found to lack thermal robustness, losing most of their initial weight between 300-600 °C under either N_2 or O_2. Heating the samples to 1000 °C revealed weight losses that correspond to the diamine chain length; the highest molecular weight diamines afforded copolymers that exhibited the greatest overall weight loss. However, the products derived from 1,12-diaminododecane (**1d** and **2d**) were also the most thermally robust at temperatures of up to 300 °C. Under O_2, **1a-1f** and **2a-2f** exhibited clear phase transitions in the first DSC cycle that correspond to temperatures of significant weight loss, features that were not observed under N_2. Analysis of samples that had been heated to 1000 °C by powder X-ray diffraction revealed amorphous material with limited formation of quartz under N_2 and cristobalite under O_2.

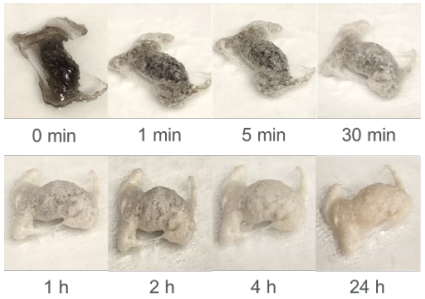

Fig. 2 Images showing the aging of silane diamine **1a** in air over the course of 24 h (27% humidity).

Table 3 Molecular weight and thermal properties of **1a-1f** and **2a-2f**.

Prod.	M_w (m/z) [a]	$T_{-5\%}$ [b] (N_2, °C)	$T_{-5\%}$ [b] (O_2, °C)	Wt. Loss 1000 °C (N_2) [b]	Wt. Loss 1000 °C (O_2) [b]
1a	3079	173	183	52%	66%
1b	1507	273	272	61%	70%
1c	1049	96	174	65%	68%
1d	3397	375	371	75%	81%
1e	3110	157	126	78%	80%
1f	3036	206	262	76%	82%
2a	2251	226	206	68%	71%
2b	1694	117	180	77%	76%
2c	1512	289	179	78%	79%
2d	2826	303	314	83%	84%
2e	2230	157	126	82%	80%
2f	2851	237	206	89%	85%

[a] Highest discernible distribution in the product wash observed by MALDI-TOF mass spectrometry. [b] Determined by TGA (25-1000 °C).

Leading Dehydrocoupling Activity. Greater than 99% diamine conversion was observed for each trial in **Table 1** and **Table 2**, giving rise to substrate utilisation TOFs of 66.7 h^{-1} and Si–N dehydrocoupling TOFs of at least 133 h^{-1} (since polymerisation requires the silylation of two or more N–H bonds per diamine).[19] To evaluate the maximum activity of the catalyst, the neat dehydrocoupling of ethylenediamine and phenylsilane was conducted in the presence of 0.01 mol% **1** and mesitylene as an internal standard. Aliquots were collected over the course of 3 h, the catalyst was deactivated by I_2, and the percent conversion was determined by integrating the starting amine and internal standard ^{1}H NMR resonances. For illustrative purposes, images of this experiment as a function of time are provided in **Fig. 3**.

Notably, 30% of the ethylenediamine was consumed after 10 s of catalysis, which equates to a substrate utilisation TOF of 300 s^{-1}. The N–H bond silylation TOF cannot be estimated from this experiment since crosslinking did not reach completion; however, it is likely to be higher than 300 s^{-1} since each diamine can react up to four times. After 30 min, 99% conversion was noted (**Table S2**), which equates to turnover numbers (TONs) of 9900 based on ethylenediamine consumption and at least 19800 based on N–H bond dehydrocoupling. Vigorous H_2 gas evolution was observed after 1 min, which continued to intensify, followed by blackening of the solution after 3 min (**Fig. 3**). At this point of the reaction, we believe that the catalyst is being converted into manganese nanoparticles that become dispersed throughout the matrix.

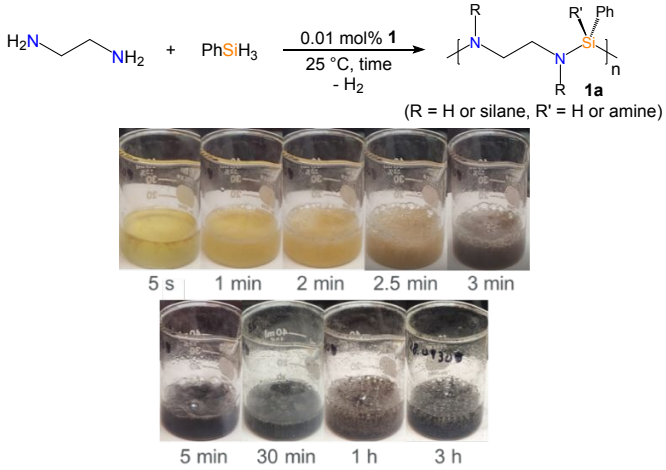

Fig. 3 Images showing the dehydrocoupling of ethylenediamine and phenylsilane using 0.01 mol% of **1** over the course of 3 h.

Swelling of Silane Diamine Networks. The ability of silane diamine networks to absorb volatile organic compounds has not been described, although this is an application of interest to the construction industry.[28] During the workup of solid **1b**-**1d** and **2b**-**2d**, it became apparent that these materials were absorbing the reaction solvent and determining their dry weight required hours of vacuum exposure. Using dry **1b** as a representative example, its ability to absorb toluene, THF, Et_2O, and pentane was evaluated. Fully submerging a 25 mg sample of **1b** in toluene for 24 h, allowing it to dry on a Kimwipe, and reweighing it revealed an increase in mass to 90.6 mg (m_1/m_0 = 3.62, **Table 4**, Entry 1). Repeating this procedure revealed a slightly higher wet mass (99.1 mg) after a 3 day soak. Compound **1b** was found to absorb a comparable quantity of Et_2O and less pentane over the same timeframes. However, it was found to be a particularly effective scavenger of THF, swelling to 4.4× its original mass after a 1 day soak, and 6.2× its original mass after a 3 day soak.

Therefore, we sought to explore the importance of diamine linker chain length while optimizing THF absorption capacity. Following the same procedure described for **1b**, networks **1a** and **1c**-**1f** were subjected to a 1 day THF soak (**Table 5**). Compound **1a** was found to swell less than those with longer chain aliphatic diamines (**1b**-**1d**) and **1d** was particularly effective at absorbing THF, swelling to 7.7× its original mass. Although **1e** and **1f** possess spacer lengths that are comparable to the 1,12-diaminododecane linkers of **1d**, these materials appear to be far less effective at absorbing THF due to their ether functionalities.

Table 4 Swelling of **1b** in a variety of organic solvents at room temperature.[a]

Entry	Dry mass (m_0)	Solv.	Wet mass 1 d (m_1)	Wet mass 3 d (m_3)	m_1/m_0	m_3/m_0
1	25.0	C_7H_8	90.6	99.1	3.62	3.96
2	23.6	THF	104.5	146.4	4.43	6.20
3	13.5	Et_2O	52.4	54.0	3.88	4.00
4	38.5	C_5H_{12}	84.1	88.5	2.18	2.30

[a] All masses in mg. Wet masses determined after removing the solvent from submerged **1b**, placing the solid on a tissue wipe, and allowing excess liquid to absorb prior to weighing.

Table 5 Swelling of **1a-1f** in THF at room temperature.[a]

Network	Dry mass (m_0)	Wet mass 1 d (m_1)	m_1/m_0
1a	23.2	59.6	2.57
1b	23.6	104.5	4.43
1c	38.5	186.3	4.84
1d	105.4	806.7	7.65
1e	53.9	95.2	1.76
1f	56.7	134.2	2.37

[a] All masses in mg. Wet masses determined after removing the solvent from submerged silane diamine network, placing the solid on a tissue wipe, and allowing excess liquid to absorb prior to weighing.

Given its effectiveness for absorbing THF, efforts were then made to recover and reuse **1d** after the first absorption cycle in **Table 5**. Notably, the complete removal of THF to achieve a dry weight of recovered **1d** required heating the swelled material for 2 days under vacuum at 60 °C. In the process, 87% of the original mass was recovered (92.0 mg vs. 105.4 mg, **Table 6**), which was again used to absorb THF during a 1 day soak. This process was repeated until four cycles of THF absorption and desorption were demonstrated. Notably, the absorption capacity of **1d** decreased after the first cycle of heating to 60 °C under vacuum (7.7× to 5.2×), suggesting that this process induces partial decomposition or rearrangement of the network structure. Although the recovered dry weight continued to decline in cycles 3 and 4 (78.6 and 62.8 mg, respectively), the material continued to absorb more than 5× its mass in THF.

Table 6 Regeneration and reuse of **1d** for THF absorption at room temperature.[a]

Cycle	Dry mass (m_0)	Wet mass 1 d (m_1)	m_1/m_0
1	105.4	806.7	7.65
2	92.0	481.1	5.22
3	78.6	328.3	5.45
4	62.8	346.5	5.52

[a] All masses in mg. Wet masses determined after removing the solvent from submerged silane diamine network, placing the solid on a tissue wipe, and allowing excess liquid to absorb prior to weighing.

The propensity of silicon-containing polymers to swell in the presence of hydrocarbon solvents including cyclohexane[29] and benzene[30] has long been known, although much of the work in this area[31-33] focused on verifying the Flory-Rehner assumptions for the free energy changes accompanying absorption.[34,35] Pushing this feature to its limit has allowed for the conception of superhydrophobic activated carbon[36] or melamine[37] sponges coated with polydimethylsiloxane, which have been found to absorb approximately 60× and 90× their original weight in THF, respectively. Conceptually, the closest material related to silane diamine networks that has been used in a solvent absorption study was reported by Kyne and Webster in 2022.[38] In the process of dehydrocoupling α,ω-diols with silanes using [(2,6-^{i}Pr$_2$^{Ph}BDI)Fe(μ-H)]$_2$, a polymer prepared from phenylsilane and 1,8-octandiol had a propensity to swell upon benzene, toluene, or THF addition. After 2 days in toluene, it reached 2.2× its original mass, modestly lower than the swelling observed for **1b** after 1 day in toluene (3.6×, **Table 4**).

Comparing Organopolysilazanes and Silane Diamine Polymers. As discussed earlier, organopolysilazanes are widely used in the automotive, aerospace, architecture, and marine industries to prevent corrosion and fouling. Since Me_2SiCl_2 and $MeSiHCl_2$ can be obtained inexpensively and at scale through the direct process (reaction of elemental Si with MeCl),[39] today's leading organopolysilazane formulations are prepared by adding NH_3 to a mixture of those precursors to generate ammonium chloride and silazane polymers that feature linear and cyclic structure (**Fig. 4a**). When applied to a surface and allowed to hydrolyse in air, these pure polysilazanes release NH_3 as siloxane linkages form. However, the crosslink density remains low due to the methyl substitution of silicon, and thermal curing at 130 °C for 4 h is required.[40] This is not ideal for many applications, so 3-triethoxy-1-propanamine is often added to promote curing at ambient temperature. This additive displaces NH_3 from the polysilazane, and while incorporated within the polymer, its silyl ethers can be hydrolysed to enhance crosslinking through the loss of ethanol and siloxane formation. Higher concentrations of 3-triethoxy-1-propanamine allow for faster curing times; for example, one popular formulation dries to the touch within 30 min at room temperature at 50% humidity to provide coatings that are approximately 10 μm thick (the coatings continue to cure over the course of weeks as moisture penetrates).[41] The supplier declined to engage following our initial request to procure this product and compare it to the silane diamine solutions discussed below, which may have been viewed as a competing technology. However, this particular coating has recently been applied to copper,[42] providing an opportunity for comparison.

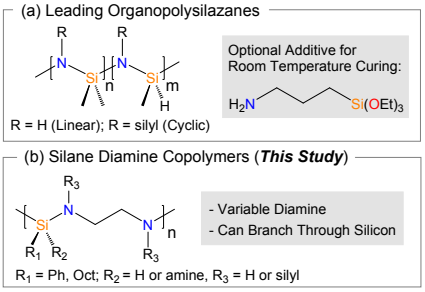

Fig. 4 Structural differences between (a) organopolysilazane coatings and (b) silane diamine alternatives.

Adding to the benefits of their halogen-free synthesis, the silane diamine combinations in **Table 1** and **Table 2** were hypothesized to feature structural differences that might be beneficial for coatings applications. For example, since they can be prepared with diamine linkers of varying chain length, the hydrophobicity of the polymer could be tuned to guide the rate of hydrolysis. Moreover, the ability of primary silanes to dehydrocouple to three amine functionalities might allow for crosslinking comparable to what is achieved when the three silyl ether functionalities of 3-triethoxy-1-propanamine are hydrolysed. The diamines chosen for this study also feature aliphatic chains that are comparable to the propylene chain of 3-triethoxy-1-propanamine, meaning that partial silane diamine hydrolysis might afford coatings similar to those obtained from commercial formulations.

Application of Silane Diamine Coatings. The networks in **Table 1** and **Table 2** cannot themselves be applied as coatings since they were purposely crosslinked into solids at high substrate concentrations (in some cases neat) to facilitate their isolation and characterization. Therefore, we sought to prepare solutions featuring low molecular weight silane diamine copolymers that could be deposited onto a surface. Accordingly, a 10% by wt. solution of ethylenediamine and phenylsilane in THF was polymerized using 0.5 mol% **1** over the course of 1 h. Copper tape was then dip-coated once into this solution of **1a** and the residual THF was allowed to evaporate under inert atmosphere over 12 h. In a similar fashion, freshly prepared 10% by wt. solutions of **1c** and **1e** were prepared by dehydrocoupling 1,6-hexanediamine and 2,2'-(ethylenedioxy)-bis(ethylamine) to $PhSiH_3$, respectively, for 1 h in THF at 60 °C. These solutions were then used for the dip-coating of copper tape that was allowed to dry under nitrogen for 12 h.

To compare how diamine chain length affects the properties of the deposited coatings, all three samples were placed in an airtight container, removed from the glovebox, and then quickly sputter coated with gold and transferred to a scanning electron microscope specimen holder in an effort to minimize air exposure. The morphology and composition of the **1a**, **1c**, and **1e** coatings on copper were then analysed by scanning electron microscopy (SEM) and energy-dispersive X-ray spectroscopy (EDX) at "0 days" of air exposure. This analysis was repeated after the coatings were allowed to cure for 1 day and 3 days in air featuring 33-42% humidity, yielding the 1000× magnification images in **Fig. 5**.

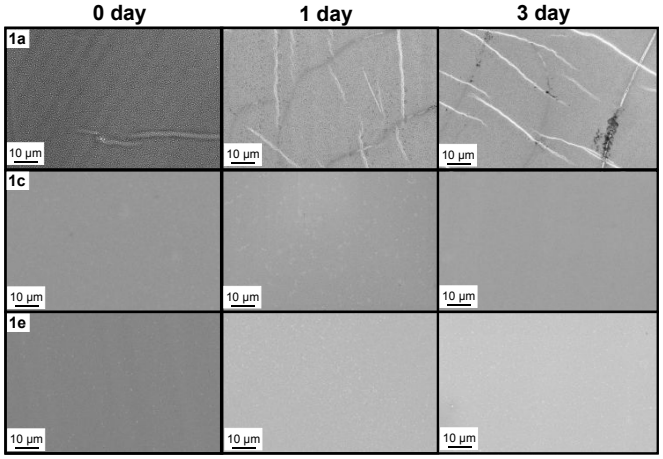

Fig. 5 SEM images of copper tape dip-coated with **1a** (top), **1c** (middle), and **1e** (bottom) at 1000× magnification at 0 day, 1 day, and 3 days of curing in air.

At 0 day with less than 3 min of air exposure, the coating of **1a** appeared to be moist (**Fig. S64**), but relatively uniform and free of cracks at 1000× magnification. However, it was also covered with spherical patterns 200-300 nm in diameter with ridges lightly dispersed across the surface. Upon analysis at 5000× magnification (**Fig. 6**), these ridges were found to feature a high density of distorted spheres that appear to be emanating from the surface. Moreover, EDX analysis revealed a weaker Cu background signature and a higher density of C and N in the location of the ridges relative to the bulk material (**Fig. S65-66**). These observations suggest that the hydrolytic liberation of ethylenediamine from the coating of **1a** occurs quickly during sample preparation, which is consistent with the bulk hydrolysis of solid **1a** shown in **Fig. 2**.

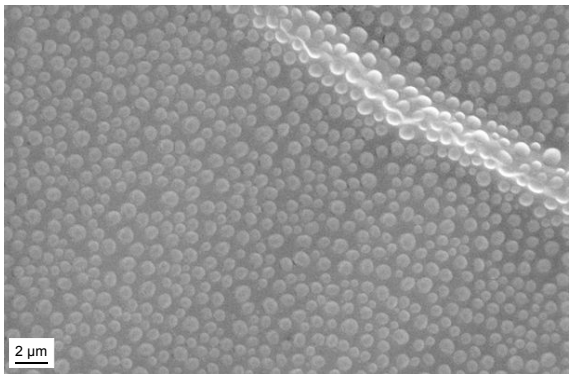

Fig. 6 SEM image of copper tape dip-coated with **1a** at 0 days of air exposure and 5000× magnification.

After allowing this coating of **1a** to cure in air for 1 day, SEM images revealed the spherical patterns that were originally present and a significant increase in the prevalence of ridges (**Fig. 5**) and cracks throughout the surface (**Fig. S64**). Cracks 2.0 µm deep (the coating thickness) were found to form upon ridge collapse, and after 3 days of curing, the coating was fractured throughout even though it did not appear so to the naked eye. These features are consistent with the continued loss of subsurface diamine units due to hydrolysis, suggesting that ethylenediamine is a poor choice of linker for silane diamine coatings since its short alkylene chain imparts a relative lack of hydrophobicity. Although ethylenediamine has a boiling point of 118 °C, its vapor pressure is 10 torr at 20 °C, which allows it to evolve from the material once hydrolysis occurs. Ammonia quickly evolves upon commercial organopolysilazane curing, but bubbling is not observed,[42] possibly because it is a gas rather than liquid under standard conditions.

The SEM analysis of **1c** coated tape at 0 day revealed a smooth and uniform coating that was free of spherical patterns and cracks, while the coating of **1e** was found to possess spherical imperfections reminiscent of those noted for the **1a** tape (**Fig. 5**). Moreover, after 1 day and 3 days of curing in air, the coating of **1c** remained intact with relatively minor imperfections while the coating of **1e** became riddled with 200 nm spheres (**Fig. 7**) upon cracking (**Fig. S64**). Notably, the coatings of **1a** and **1e** are derived from liquid diamines (which give rise to bubbles or pooling as droplets) while **1c** releases a room temperature solid, 1,6-hexanediamine. Since this diamine appears to remain embedded upon curing, while minimally disrupting the coating texture, one possible advantage of applying **1c** over an organopolysilazane is that curing would not expose the consumer to gaseous NH_3.

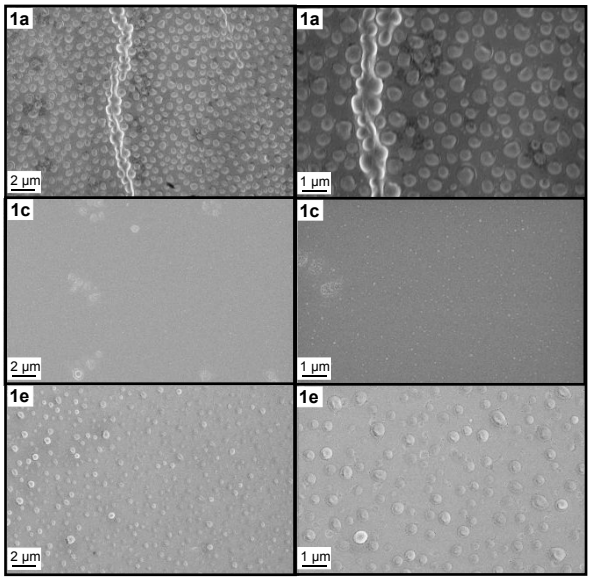

Fig. 7 SEM images of copper tape dip-coated with **1a** (top), **1c** (middle), and **1e** (bottom) after 1 day of curing in air at 5000× magnification (left) and 10000× magnification (right).

To evaluate the effect of silane substitution, the same coating depositions and analyses were repeated for freshly prepared 10% by wt. solutions of **1**-dehydrocoupled **2a**, **2c**, and **2e** in THF. Upon drying the coatings for 12 h under inert atmosphere, SEM images and EDX data were collected for each sample at 0 day, 1 day, and 3 days of exposure to air featuring 55-63% humidity. It was immediately noticed that the coating of **2a** was uniform over the striated surface of the copper tape with modest sphere formation and similar appearance to organopolysilazane coated copper (**Fig. 8**).[42] Analogous striation was observed for the coatings of **2c** and **2e**, an indication that

the $OctSiH_3$ derived coatings were thinner than those prepared from $PhSiH_3$. Since the coatings of **1a** and **1e** were estimated to be 2.0 and 0.6 µm thick, respectively, relative EDX copper signatures allowed for approximation of the **1c** (2.7 µm), **2a** (0.4 µm), **2c** (0.1 µm), and **2e** (0.2 µm) coating thicknesses [Cu%: **1a**, 26.0; **1c**, 19.2; **1e**, 24.5; **2a**, 55.6; **2c**, 88.1; **2e**, 76.9]. Residual Mn was not observed by EDX within the detection limit of the instrument.

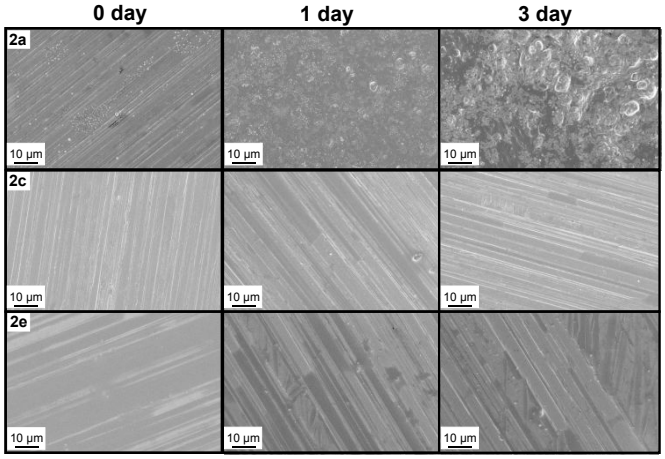

Fig. 8 SEM images of copper tape dip-coated with **2a** (top), **2c** (middle), and **2e** (bottom) at 1000× magnification at 0 day, 1 day, and 3 days of curing in air.

After 1 day of curing in air, SEM revealed that the coating of **2a** degraded considerably, hydrolyzing to generate crevasses and plateaus covered by what appears to be ethylenediamine droplets (**Fig. 9**). This process continued to worsen after 3 days of curing (**Fig. 8**). Concurrent analysis of **2c** and **2e** revealed that these coatings remained largely intact after 1 day and 3 days of exposure to air featuring 55-63% humidity, although depressions are observable for **2c** at 10000× magnification (**Fig. 9**). These observations offer insight that may guide future silane diamine coating development; the aliphatic chains of octylsilane impart hydrophobicity to the coating relative to aryl groups, as evidenced by the slow loss of ethylenediamine from **2a** relative to **1a**. Moreover, less volatile, longer chain diamines appear to be more appropriate linkers for this application.

Importantly, several limitations were also discovered during these trials. First, commercial organopolysilazane formulations are often undiluted, and dip-coating can afford coatings that are 10 µm thick.[41] The silane diamine coatings studied here are far thinner, especially those derived from octylsilane, limiting their potential for anti-corrosion applications. A preliminary attempt to build a thicker coating using a 20% by wt. solution of **1c** (the thickest coating from the trials) and dip-coating copper tape into it 3× afforded a rugged, feathered surface that was not desired (**Fig. S68**). Second, the as prepared solutions appear to have a relatively short shelf-life. Because **1**-catalyzed silane diamine coupling continues as the solutions are stored at room temperature, gels form in approximately 3 d using phenylsilane. Our efforts suggest there is a tradeoff between coating thickness and shelf-life; phenylsilane-derived coatings **1a**, **1c**, and **1e** were considerably thicker than coatings of **2a**, **2c**, and **2e** due to more effective dehydrocoupling, but continued **1a**, **1c**, and **1e** crosslinking eventually resulted in solid formation. In order to rival the shelf-life of commercial organopolysilazanes (18 months)[41] a catalyst inhibitor would need to be added at the desired stage of dehydrocoupling. Third, the coatings of **1a**, **1c**, and **1e** remained tacky after curing at room temperature for 3 days in air. This was not noted for the thinner octylsilane coatings. Therefore, higher temperatures or a higher degree of crosslinking might be needed, a limitation that also exists for commercial organopolysilazanes.[40] Although they lie beyond the scope of this study, additional factors that can allow for the optimization of silane diamine coatings include the nature, loading, activity, and lifetime of the catalyst, precursor choice and concentration, deposition method, as well as the duration and conditions of drying and curing.

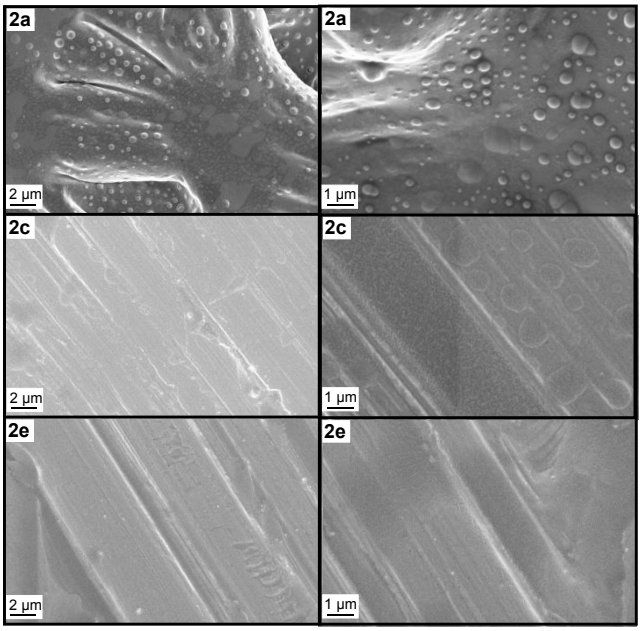

Fig. 9 SEM images of copper tape dip-coated with **2a** (top), **2c** (middle), and **2e** (bottom) after 1 day of curing in air at 5000× magnification (left) and 10000× magnification (right).

Conclusions

This study demonstrated that the Mn-catalysed coupling of primary silanes to diamines can allow for the efficient and halogen-free preparation of silane diamine networks. Upon lowering the loading of $[(^{2,6\text{-}i\text{Pr}_2\text{Ph}}\text{BDI})\text{Mn}(\mu\text{-H})]_2$ (**1**) to 0.01 mol%, diamine utilisation TOFs of up to 300 s^{-1} were achieved, the highest Si–N dehydrocoupling activity reported to date. The products of these initial reactions feature a high degree of crosslinking and were found to swell when exposed to organic solvents, most notably THF. The network generated via 1,12-diaminododecane and phenylsilane dehydrocoupling (**1d**) was found to absorb 7.7× its mass in THF after a 1 day soak and was capable of being regenerated and reused 4×. The ability of the catalyst to yield copolymers with varied diamine chain lengths also allowed us to prepare lightly crosslinked solutions that could be applied as coatings to copper and evaluated upon hydrolysis. Coatings featuring 1,6-hexanediamine linkers best

retained their integrity upon curing in air for 3 days at ambient temperature and offered the closest comparison to structurally-related organopolysilazane formulations. Potential limitations of silane diamine coatings that may guide future inquiry were also elucidated. In this study, they included the need to prepare solutions (which did not allow for coatings of optimal thickness), ongoing dehydrocoupling (which resulted in short shelf life), and in the case of phenylsilane, insufficient drying (which led to undesired tackiness).

Acknowledgements

This material is based upon work supported by the National Science Foundation under Grant No. 2154359. We acknowledge the use of facilities within the Eyring Materials Center at Arizona State University, supported in part by NNCI-ECCS-1542160.

Conflicts of interest

T.T.N. and R.J.T. retain rights to **1** and its use to make silane diamine copolymers through U.S. Patent No. 11,273,432 (**2022**).

Notes and references

1 E. Kroke, Y.-L. Li, C. Konetschny, E. Lecomte, C. Fasel and R. Riedel, *Mat. Sci. Eng. R*, 2000, **26**, 97-199.
2 P. Colombo, G. Mera, R. Riedel and G. D. Sorarù, *J. Am. Ceram. Soc.*, 2010, **93**, 1805-1837.
3 Y. Kuo, *Vacuum*, 1998, **51**, 741-745.
4 A. El amrani, I. Menous, L. Mahiou, R. Radjine, A. Touati and A. Lefgoum, *Renew. Energ.* 2008, **33**, 2289-2293.
5 R. M. Laine, Y. D. Blum, D. Tse and R. Glaser, *ACS Symp. Ser.,* 1988, **360**, 124-142.
6 H. Krannich, R. Mehnert, J. Reiser and S. Weseloh, US Patent Appl. No. 2010/0075057 A1.
7 S. Marceaux, C. Bressy, F.-X. Perrin, C. Martin and A. Margaillan, *Prog. Org. Coat.* 2014, **77**, 1919-1928.
8 T. D. H. Nguyen, F.-X. Perrin and D. L. Nguyen, *J. Nanotechnol.* 2013, **4**, 671-677.
9 W. Fink, *Helv. Chim. Acta*, 1968, **51**, 954-974.
10 A. Stock and K. Somieski, *Ber. Dtsch. Chem. Ges.* 1921, **54**, 740.
11 S. D. Brewer and C. P. Haber, *J. Am. Chem. Soc.* 1948, **70**, 3888-3891.
12 H. Q. Liu and J. F. Harrod, *Organometallics*, 1992, **11**, 822-827.
13 B. E. Leland, J. Mondal and R. J. Trovitch, *Chem. Commun.* 2023, **59**, 3665-3684.
14 C. Bellini, C. Orione, J.-F. Carpentier and Y. Sarazin, *Angew. Chem. Int. Ed.* 2016, **55**, 3744-3748.
15 C. Bellini, T. Roisnel, J.-F. Carpentier, S. Tobisch and Y. Sarazin, *Chem. Eur. J.* 2016, **22**, 15733-15743.
16 L. J. Morris, G. R. Whittell, J.-C. Eloi, M. F. Mahon, F. Marken, I. Manners and M. S. Hill, *Organometallics*, 2019, **38**, 3629-3648.
17 D. Gasperini, A. K. King, N. T. Coles, M. F. Mahon and R. L. Webster, *ACS Catal.* 2020, **10**, 6102-6112.
18 M.-M. Liu, Y. Xu and C. He, *J. Am. Chem. Soc.,* 2023, **145**, 11727-11734.
19 A. Sharma, R. H. Bean, T. E. Long and R. J. Trovitch, *ACS Sustainable Chem. Eng.,* 2023, **11**, 11172-11180.
20 P. Rios, M. Rosello-Merino, O. Rivada-Wheelaghan, J. Borge, J. Lopez-Serrano and S. Conejero, *Chem. Commun.*, 2018, **54**, 619-622.
21 T. K. Mukhopadhyay, M. Flores, T. L. Groy and R. J. Trovitch, *Chem. Sci.* 2018, **9**, 7673-7680.
22 C. Oh, J. Siewe, T. T. Nguyen, A. Kawamura, M. Flores, T. L. Groy, J. S. Anderson, R. J. Trovitch and M.-H. Baik, *Dalton Trans.*, 2020, **49**, 14463-14474.
23 T. T. Nguyen, J.-H. Kim, S. Kim, C. Oh, M. Flores, T. L. Groy, M.-H. Baik and R. J. Trovitch, *Chem. Commun.* 2020, **56**, 3959-3962.
24 T. T. Nguyen, T. K. Mukhopadhyay, S. N. MacMillan, M. T. Janicke and R. J. Trovitch, *ACS Sustainable Chem. Eng.*, 2022, **10**, 4218-4226.
25 K. Suzuki, T. Okamura, T. Okayasu and T. Vom Stein, World Intellectual Property Organization Patent Appl. No. 2022/084022 A1.
26 Y. Liu, J.-M. Girard, P. Zhang, F. Qin, G. Itov, F. Marchegiani, T. J. Larrabee, V. R. Pallem. US Patent Appl. No. 2023/0095074 A1.
27 A. L. Smith, *Spectrochimica Acta*, 1960, **16**, 87-105.
28 K. W. Shah and W. Li, *Nanomaterials*, 2019, **9**, 910.
29 N. Kuwahara, T. Okazawa and M. Kaneko, *J. Polym. Sci. C* 1968, **23**, 543-553.
30 P. J. Flory and H. Shih, *Macromolecules*, 1972, **5**, 761-766.
31 R. W. Brontman and B. E. Eichinger, *Macromolecules*, 1981, **14**, 1445-1448.
32 R. W. Brontman and B. E. Eichinger, *Macromolecules*, 1982, **15**, 535-537.
33 N. A. Neuburger and B. E. Eichinger, *Macromolecules*, 1988, **21**, 3060-3070.
34 P. J. Flory and J. Rehner, Jr., *J. Chem. Phys.* 1943, **11**, 521-526.
35 P. J. Flory, *J. Chem. Phys.* 1950, **18**, 108-111.
36 H. Sun, A. Li, Z. Zhu, W. Liang, X. Zhao, P. La and W. Deng, *ChemSusChem* 2013, **6**, 1057-1062.
37 V. H. Pham and J. H. Dickerson, *ACS Appl. Mater. Interfaces*, 2014, **6**, 14181-14188.
38 M. A. Farcaş-Johnson, S. H. Kyne, R. L. Webster, *Chem. Eur. J.* 2022, e202201642.
39 E. G. Rochow, *Inorg. Synth.* 1950, **3**, 56-58.
40 Durazane® 1033, 1066, 1085, Technical Datasheet, EMD Performance Materials of Merck KGaA, Darmstadt, Germany, February, 2021.
41 Durazane® 1500 rapid cure, Technical Datasheet, EMD Performance Materials of Merck KGaA, Darmstadt, Germany, February, 2021.
42 Ramdé, T.; Rossi, S.; Fedel, M.; Bonou, L. *J. Appl. Electrochem.* 2023, **53**, 797-809.

